



On the Consistency of Scale Among Experiments, Theory, and Simulation

James E. McClure¹, Amanda L. Dye², Cass T. Miller², and William G. Gray³

¹Advanced Research Computing, Virginia Tech, Blacksburg, Virginia 24601-0123, USA

²Department of Environmental Sciences and Engineering, University of North Carolina, Chapel Hill, North Carolina 27599-7431

³Curriculum for the Environment and Ecology, University of North Carolina, Chapel Hill, North Carolina 27599-3135

Correspondence to: William G. Gray (GrayWG@unc.edu)

Abstract. The career of Professor Eric F. Wood has focused on the resolution of problems of scale in hydrologic systems. Within this context, we consider an evolving approach known as the thermodynamically constrained averaging theory (TCAT), which has broad applicability to hydrology. Specifically, we consider the case of modeling of two-fluid-phase flow in porous media. Two-fluid flow processes in the subsurface are fundamentally important for a wide range of hydrologic processes, including the transport of water and air in the vadose zone and geological carbon sequestration. Mathematical models that describe these complex processes have long relied on empirical approaches that neglect important aspects of the system behavior. New data sources make it possible to access the true geometry of geologic materials and directly measure previously inaccessible quantities. This information can be exploited to support a new generation of theoretical models that are constructed based on rigorous multiscale principles for thermodynamics and continuum mechanics. The challenges to constructing a mature model are shown to involve issues of scale, consistency requirements, appropriate representation of operative physical mechanisms at the target scale of the model, and a robust structure to support model evaluation, validation, and refinement. We apply TCAT to perform physics-based data assimilation to understand how the internal behavior influences the macroscale state of two-fluid porous medium systems. Examples of a microfluidic experimental method and a lattice Boltzmann simulation method are used to examine a key deficiency associated with standard approaches. In a hydrologic process such as evaporation, the water content will ultimately be reduced below the irreducible wetting phase saturation determined from experiments. This is problematic since the derived closure relationships cannot predict the associated capillary pressures for these states. In this work, we demonstrate that the irreducible wetting-phase saturation is an artifact of the experimental design, caused by the fact that the boundary pressure difference does not approximate the true capillary pressure. Using averaging methods, we measure the true capillary pressure for fluid configurations at and below the irreducible wetting phase saturation. Results of our analysis include a state function for the capillary pressure expressed as a function of fluid saturation and interfacial area.

1 Introduction

The years spanning the career of Eric F. Wood have witnessed a remarkable development in the ability to study experimentally the elements that comprise the hydrologic universe. The subsurface is a porous medium system that receives experimental



attention designed to identify the small-scale fluid distributions within the solid matrix, intermediate scale behavior through laboratory study, and also the response of an aquifer to imposed forces (e.g., Wildenschild and Sheppard, 2013; Dye et al., 2015; Alizadeh and Piri, 2014; Knödel et al., 2007). Turbulence in surface flows and its impact in rivers, estuaries, and oceans for flow, sediment transport, and dissolved species transport is examined using a broad range of experimental techniques (e.g.,

5 Bradshaw, 1971; Chanson, 2009; D'Asaro, 2014; Bernard and Wallace, 2002). Atmospheric experiments designed to support theoretical models of turbulence, typically using lidar systems, and to gain insight into turbulence structures have also generated large quantities of data (Sathe and Mann, 2013; Collins et al., 2015; Fuentes et al., 2014). Other studies involve examination of snow pack, desertification, and changes in land usage (Deems et al., 2013; Hermann and Sop, 2016; Lillesand et al., 2015; Nickerson et al., 2013).

10 Complementing the advancing ability of experimental study is the development of simulation tools for various aspects of hydrologic systems that make use of advanced computer technology (e.g., Miller et al., 2013; Flint et al., 2013; Kauffeldt et al., 2016; Paiva et al., 2011; Dietrich et al., 2013; Zhou and Li, 2011; Miller et al., 1998; Bauer et al., 2015; Dudhia, 2014). These models of watersheds, rivers and estuaries, and subsurface regions usually make use of traditional equations with the advances occurring through the ability of modern computer architecture to handle larger problems using parallel computing and more

15 elegant, efficient graphical user interfaces.

A third element of advancing modeling of water resources systems is the development of theory that accounts for physical processes. On one hand, forming theoretical advances can be viewed as the standard challenge of developing closure relations for dissipative processes. However, the need to pose these closure relations at scales that are consistent with the scales at which the problems have been formulated creates a need for a variety of constitutive proposals. Furthermore, consistency of models

20 requires that equation formulations be consistent across scales such that variables developed at a smaller scale can inform the equations employed at a larger scale. Overall, these considerations lead to identifying scale and scaling behavior in both time and space as important challenges in posing models (Wood, 1995; Wang et al., 2006; Skøien et al., 2003; Pechlivanidis et al., 2011; Gleeson and Paszkowski, 2014; Gentine et al., 2012; Blöschl, 2001).

In an era of unprecedented data generation, a specter haunts the scientific landscape: the pervasive application of statistical

25 methods to misinterpret complex physical phenomena. In the face of this challenge, multiscale averaging theory offers a glimmer of hope. Opportunities to apply theoretical methods for physics-based data assimilation have never been more evident. The challenge of performing meaningful theoretical, experimental, and computational analyses is constrained by the need to ensure that the length and time scales of quantities arising in each approach can be related. The scales of experimental data, variables appearing in equations, and computed quantities must be the same if they are to be compared in any meaningful

30 way. As a prerequisite for this to happen, data generated by any of the methods must be consistent across the range of scales considered (Ly et al., 2013; Kauffeldt et al., 2013).

While the desire for consistency across scales and approaches is conceptually simple to understand, it has proven to be a difficult objective to meet in practice. The change in scale of conservation and balance equations can be accomplished rather easily. The problem with applying these equations lies in the aforementioned need to average some intensive variables,

35 the requirement that closure conditions be proposed at the larger scale, and the need to account for the dynamics of new



quantities that arise in the change of scale. Without accounting for all of these items properly, models are doomed to fail. An essential element in ensuring success is the averaging of thermodynamic relations to the larger scale (Gray and Miller, 2013). This provides linkage of variables across scales and also ensures that all physical processes are properly accounted for. For modeling rainfall-runoff processes, Wood et al. (1988) proposed the use of a representative elementary area as a portion of a watershed over which averaging can occur to develop a model. This idea was extended and applied by (Blöschl et al., 1995). Subsequently, (Reggiani et al., 1998) proposed treating a hydrologic system as a collection of interconnected lumped elements. The lumping was accomplished by integration over individual portions of the system with distinct properties, e.g., aquifers, streams, channels. This effort did not include integration of thermodynamic relations, and as a result did not properly account for the impact of gravitational potential in driving flow between system elements. An effort to address this shortcoming by a somewhat *ad hoc* introduction of gravitational forces (Reggiani et al., 1999) was only partially successful.

Similar challenges have confronted the modeling of porous medium systems. Special challenges have been encountered for two-fluid-phase flow, where upscaling leads to the introduction of quantities such as specific interfacial areas and specific common curve lengths. Modeling of multiscale porous medium systems can also benefit from thermodynamics that is scale-consistent and included naturally as a part of the process. As a result of these challenges, most efforts to model multiscale, multiphase porous medium systems do not have thermodynamic constraints and full-scale consistency that is sought in mature models. The thermodynamically constrained averaging theory (TCAT) approach is relatively refined and does provide a means to model effectively systems that are inherently multiscale in nature and to link disparate length scales, while representing the essential physics naturally and hierarchically with varying levels of sophistication. However, realizing these scale-consistent attributes requires new approaches, new equations of state, novel parameterizations, and, as with any new model, evaluation and validation.

2 Objectives

The overall goal of this work is to examine issues of scale consistency for two-fluid-phase porous medium systems. The specific objectives of this work are:

- to review efforts to resolve critical issues of scale for two-fluid-phase flow in porous media;
- to formulate microscale and macroscale descriptions of state variables important for traditional and evolving descriptions of capillary pressure;
- to determine state variables for capillary pressure using both experimental and computational approaches;
- to compare a traditional state equation approximation approaches with a carefully formulated approach based in multi-scale TCAT theory;
- to demonstrate the limitations of traditional state equation approaches for capillary pressure; and
- to examine the uniqueness of alternative state equation formulations.



3 Background

As efforts to model and link hydrologic elements in models advance, the ability to address scales effectively will become essential. For porous media, methods such as averaging, mixture theory, percolation theory, and homogenization have been employed to transform governing system equations from smaller to larger length scales (Hornung, 1997; Panfilov, 2000; Cushman, 1997). The goal of such approaches is to transform small-scale data to a larger scale such that it can be used to inform models that have been obtained by consistent transformation of conservation and balance equations across scales.

Averaging procedures have been used for analysis of porous media for approximately 50 years (e.g., Bear, 1972; Anderson and Jackson, 1967; Whitaker, 1986, 1999; Marle, 1967). The methods of averaging can be applied to single-phase systems as well as to multiphase systems. Success in the development of averaging equations for single-fluid-phase porous media to obtain equations such as Darcy's Law has been achieved (e.g., Bachmat and Bear, 1964; Whitaker, 1967; Gray and O'Neill, 1976). These instances did not so much derive a flow equation as show that a desired flow equation could be obtained using averaging theorems and appropriate assumptions. Thus, these early efforts did not contribute significantly to objective development of flow equations that seek to capture important physical processes. They do serve to provide a systematic framework for developing larger scale equations. Work for two or more fluid phases in porous media has proven to be more difficult and has not been as illuminating.

The problems associated with trying to model multiple fluid phases in porous media include difficulties in properly accounting for interface properties, lack of definition of macroscale intensive thermodynamic variables, failure to account for system kinematics, and representing other important physical phenomena explicitly, such as contact angles and common curve behavior. These four difficulties sometimes impact the system description in combination.

Multiple-fluid-phase porous media differ from a single-fluid-phase porous medium system by the presence of the interface between the fluids. This interface is different from a fluid-solid interface because of its dynamics. The total amount of solid surface is roughly constant, or is slowly varying, for most natural solid materials. The fluid-fluid specific interfacial area changes in response to flow in the system and redistribution of phases. The time scale of this change is between that of the pore diameter divided by flow velocity and that of pore diameter divided by solid phase movement. These specific interfacial areas are important for their extent, surface tension, and curvature. They are the location where capillary forces are present. Thus, a physically consistent model must account for mass, momentum, and energy conservation at the interfaces; a model concerned only with phase behavior cannot be successful (Gray et al., 2015). This failure is evidenced, in part, by multi-valuedness when capillary pressure is proposed to be a function only of saturation (Albers, 2014).

Intensive variables that are introduced at the macroscale without consideration of microscale precursor values are also poorly defined. For example, a range of procedures for averaging microscale temperature can be employed that will lead to different macroscale values unless the microscale temperature is constant over the averaging region. Thus, mere speculation that a macroscale value exists fails to identify how or if this value is related to unique microscale variables and most certainly does not relate the macroscale variable to microscale quantities. The absence of a theoretical relation makes it impossible to reliably relate microscale measurements to larger scale representations (Essex et al., 2007; Maugin, 1999). Further confusion arises



when pressure is proposed directly at the macroscale. Microscale capillary pressure is related to the curvature of the interface between fluid phases and does not depend on the pressures in the two phases themselves. At equilibrium, capillary pressure becomes equal to the difference between phase pressures at the interface. Macroscale proposals often specify that the capillary pressure is equal to the difference in some directly presumed quantity known as macroscale pressure, and thus ignore both interface curvature and the fact that only when evaluated at the interface is the phase pressure important. This is especially problematic when boundary pressures in an experimental cell are used to compute a so called “capillary pressure.” Note that under these common experimental conditions, regions of entrapped non-wetting phase are not in contact with the non-wetting fluid that is observed on the boundary of the system.

The importance of kinematics is recognized, at least implicitly, in modeling many systems at reduced dimensionality or when averaging over a region the system occupies. For example, in the derivation of vertically integrated shallow water flow equations, a kinematic condition on the top surface is imposed based on the condition that no fluid crosses that surface (Vreugdenhil, 1995). Macroscale kinematic equations for interfaces between fluids in the absence of porous media have been proposed in the context of boiling (Kocamustafaogullari and Ishii, 1995; Ishii et al., 2005). Despite the fact that interface reconfiguration has an important role in determining the properties and behavior of a multifluid porous medium system, attention to this feature is extremely limited (Gray and Miller, 2013; Gray et al., 2015). In some cases, models of two-fluid-phase flow in porous media have been proposed that do not account for system kinematics and also do not properly account for interfacial stress (Niessner et al., 2011), which are necessary components of physically realistic, high fidelity models.

The mixed success in posing appropriate theoretical models, making use of relevant data, and harnessing effective computer power to advance understanding of hydrologic systems is attributable to the inherent difficulty of each of these scientific activities. For progress to be made in enhancing understanding, a significant hurdle must be navigated that requires consistency among these three approaches and within each approach individually. We have found that by performing complementary microscale experimental and computational studies, we have formed a basis for being able to upscale data spatially with insights into the operative time scales for the system. The small-scale data supports our quest for larger scale closure relations and eliminates confusion about concepts such as capillary pressure as a state function and dynamic processes that cause changes in the value of capillary pressure. Key to being able to develop faithful models are consistent scale change of thermodynamic relations and implementation of appropriate kinematic relations.

4 Approach

4.1 Measures of Macroscale State

Direct upscaling can be performed based on microscale information. This upscaling provides an opportunity to explore aspects of macroscale system behavior that have previously been overlooked. Essential to this process and underpinning this exploration is the precise definition of macroscale quantities. TCAT models are derived from first-principles starting from the microscale. Microscale quantities and equations are averaged to the macroscale. Important macroscale quantities that arise, such as phase pressures, specific interfacial areas, curvatures, are defined unambiguously based on the microscale variables



and precisely defined averaging (e.g. Gray and Miller, 2014). For two-fluid-phase flow we consider the wetting phase (w), the non-wetting phase (n), and the solid phase (s) within a domain Ω . Each phase occupies part of the domain, Ω_α , where $\alpha = \{w, n, s\}$. The intersection between any two phases is an interface. The three interfaces are denoted by Ω_{wn} , Ω_{ws} , and Ω_{ns} . Finally, the common curve Ω_{wns} is defined by the juncture of all three phases. The averaged TCAT two-phase model is developed with the complete set of entities, with the index set $\mathcal{J} = \{w, n, s, wn, ws, ns, wns\} = \mathcal{J}_P \cup \mathcal{J}_I \cup \mathcal{J}_C$ chosen to include all three phases $\mathcal{J}_P = \{w, n, s\}$, the interfaces $\mathcal{J}_I = \{wn, ws, ns\}$, and the common curve $\mathcal{J}_C = \{wns\}$. Based on these identifications, the pore space is defined as the union of the domains for the two fluids $\mathcal{D}_f = \Omega_w \cup \Omega_n$.

Macroscopic quantities can be determined explicitly from microscale information based on averages. In this work, the form for averages is

$$\langle P \rangle_{\alpha, \beta} = \frac{\int_{\Omega_\alpha} P d\mathbf{r}}{\int_{\Omega_\beta} d\mathbf{r}}, \quad (1)$$

where P is the microscale quantity being averaged. The domains for integration can be the full domain Ω , the entity domains Ω_α for $\alpha \in \mathcal{J}$, or their boundary Γ_α . The boundary of an entity, Γ_α , can be sub-divided into an interior portion within the averaging volume, $\Gamma_{\alpha i}$, and an external portion, $\Gamma_{\alpha e}$, at the exterior boundary of the averaging region. Thus we note that $\Gamma_\alpha = \Gamma_{\alpha i} \cup \Gamma_{\alpha e}$ where the external boundary is simply $\Gamma_{\alpha e} = \Omega_\alpha \cap \Gamma$.

The volume fractions, specific interfacial areas, and specific common curve length are each extent measures that can be formulated as

$$\epsilon^{\bar{\alpha}} = \langle 1 \rangle_{\Omega_\alpha, \Omega}. \quad (2)$$

The volume fractions correspond to $\alpha \in \mathcal{J}_P$, specific interfacial areas correspond to $\alpha \in \mathcal{J}_I$, and the specific common curve length corresponds to $\alpha = wns$. The system porosity, ϵ , is directly related to the solid fraction volume fraction by

$$\epsilon = 1 - \epsilon^{\bar{s}}. \quad (3)$$

The wetting phase saturation, $s^{\bar{w}}$, can also be expressed in terms of the extent measures,

$$s^{\bar{w}} = \frac{\epsilon^{\bar{w}}}{1 - \epsilon^{\bar{s}}} = \frac{\epsilon^{\bar{w}}}{\epsilon}. \quad (4)$$

At the macroscale, various averages arise for the fluid pressures. For flow processes, the relevant quantity is an intrinsic average of the microscale fluid pressure, p_α , expressed as

$$p^\alpha = \langle p_\alpha \rangle_{\Omega_\alpha, \Omega_\alpha} \quad (5)$$

for $\alpha \in \mathcal{J}_f$. In most laboratory experiments fluid phase pressures are measured at the boundary of the full domain, since it is not practical to insert pressure transducers within the sample. The associated average pressure for the intersection of the boundary of the phase with the exterior of the domain is denoted as p_α^Γ where

$$p_\alpha^\Gamma = \langle p_\alpha \rangle_{\Gamma_{\alpha e}, \Gamma_{\alpha e}}, \quad (6)$$



for $\alpha \in \mathcal{J}_f$.

The capillary pressure of the two-fluid-phase system is a state function for the interface that depends on the curvature of the interface between the fluids and the surface tension. The curvature of the boundary of phase β is defined at the microscale as

$$5 \quad J_\beta = \nabla' \cdot \mathbf{n}_\beta, \quad (7)$$

where $\nabla' = (\mathbf{I} - \mathbf{n}_\beta \mathbf{n}_\beta) \cdot \nabla$ is the microscale divergence operator restricted to a surface, and \mathbf{n}_β is the outward normal vector from the β phase. Since an internal boundary is an interface, the curvature of a phase boundary is also the curvature of the interface between phases for locations within the domain. At the microscale, the capillary pressure is defined at the interface between fluid phases as

$$10 \quad p_{wn} = -\gamma_{wn} J_w, \quad (8)$$

where γ_{wn} is the interfacial tension of the wn interface. Laplace's law is a microscale equilibrium balance of forces acting on an interface that relates the capillary pressure to the difference between the microscale phase pressures evaluated at the interface with

$$p_n - p_w = -\gamma_{wn} J_w. \quad (9)$$

15 It is important to emphasize that Laplace's law applies at points on the wn interface only at equilibrium; the definition of capillary pressure given by Eq. 8 applies even when the system is not at equilibrium. Additionally, if the mass per area of the interface is non-zero, Laplace's law must be modified to account for gravitational effects. Care must be taken when extending this relationship to the macroscale.

Since the capillary pressure is defined for the interface between the two fluids, Ω_{wn} , we consider an average of the microscale
 20 curvature over this entity

$$J_w^{wn} = \langle J_w \rangle_{\Omega_{wn}, \Omega_{wn}} = -\langle J_n \rangle_{\Omega_{wn}, \Omega_{wn}}. \quad (10)$$

Similarly, the macroscale capillary pressure, p^{wn} , is an average over the interface with

$$p^{wn} = -\langle \gamma_{wn} J_w \rangle_{\Omega_{wn}, \Omega_{wn}}. \quad (11)$$

When the microscale interfacial tension is constant, this equation simplifies to

$$25 \quad p^{wn} = -\gamma^{wn} J_w^{wn}. \quad (12)$$

In the context of Eq. 9 a third pressure of interest for two-fluid-phase systems is the fluid phase pressure averaged over an interface on the boundary of the phase

$$p_\alpha^{wn} = \langle p_\alpha \rangle_{\Omega_{wn}, \Omega_{wn}}, \quad (13)$$



From the definitions of pressures provided it is clear that several different pressure measures are of interest for two-fluid systems. In general these measures will not be equivalent. Thus care is needed in analyzing the system state and in proposing relations among pressures. In general only the pressure defined by Eq. 6 is typically measured in traditional laboratory experiments, and this is often true even with state-of-the-science experiments that include high-resolution imaging. On the other hand, computational approaches provide a means to compute all of the defined measures of pressure, yielding a basis to deduce a more complete understanding of the macroscale behavior of a system than would be accessible using approaches that are only able to control and observe fluid pressures on the boundaries of the domain.

4.2 Experimental Design

Two-fluid flow experiments through porous media are typically conducted using a setup similar to the one shown in Fig. 1. A porous material, in this case a two-dimensional micromodel cell, is connected to two fluid reservoirs at opposite ends of the sample. The two fluids are referred to as wetting (w) and non-wetting (n) based on the relative affinity of the fluids toward the solid phase (s , the black region of Fig. 1). The two-dimensional micromodel was fabricated using photolithography techniques. The 500 $\mu\text{m} \times 525 \mu\text{m} \times 4.4 \mu\text{m}$ porous medium cell of the micromodel contained a distribution of cylinders, with a porosity of 0.54. The boundary reservoirs were used to inject fluid into the sample, resulting in the displacement of one fluid by the other. As depicted in Figure 1, one inlet of the cell was connected to a wetting-fluid-phase (decane) reservoir and the other to a non-wetting-fluid-phase (nitrogen gas) reservoir, with the other four boundaries being solid. A displacement experiment was performed in the micromodel depicted in Fig. 1 using the experimental methods detailed in Dye et al. (2015). This approach provides observations of equilibrium configurations of the two-fluid-phase system. The displacement experiment began by fully saturating the porous medium cell with decane through the inlet reservoir located at one end of the cell. Primary drainage was then carried out by incrementally increasing the pressure of the nitrogen reservoir, located on the opposite end of the cell. After each pressure step the system was allowed to equilibrate. The final equilibrium state for a given pressure boundary condition was determined based on the average mean curvature of the wn interface, J_w^{wn} , as determined from image analysis. After the system reached an equilibrium state, the pressure in each reservoir and an image of the cell were recorded before another incremental change in pressure step was applied. The drainage process was terminated prior to nitrogen breakthrough into the decane reservoir.

The solid geometry used in our microfluidic experiments was designed to allow for high capillary pressure at the end of primary drainage. At the wetting-fluid-phase reservoir, a layer of evenly spaced homogeneous cylinders was placed such that the gap between cylinders was uniformly small. This allowed for a large pressure difference between the fluid reservoirs, since the non-wetting fluid phase did not penetrate the wetting-fluid-phase reservoir over a wide range of pressure differences.

4.3 Computational Approach

The experimental microfluidics setup described in the previous section provides a way to perform traditional two-fluid-flow experiments and observe the internal dynamics of interface kinematics and equilibrium distributions. Microscale phase configurations can be observed directly, and averaged geometric measures can be obtained from this data. While boundary pressure

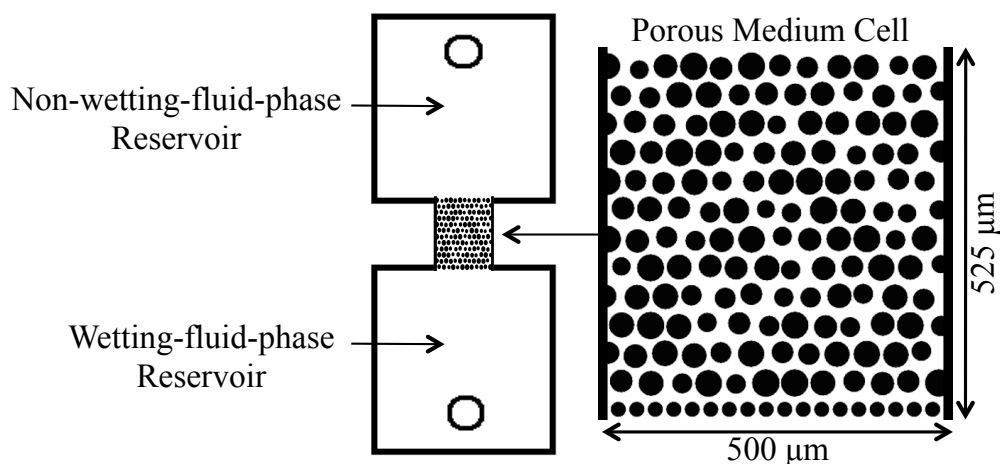


Figure 1. A depiction of the two-dimensional micromodel that was used in the displacement experiment. The solid is represented by black and the regions accessible to fluid flow by white within the porous medium cell.

values are known, the experiment does not provide a way to measure the microscale pressure field. Accurate computer simulation of the experiment can provide this information and can also be used to generate additional fluid configurations that may not be accessible experimentally. In particular, configurations below the irreducible wetting phase saturation will be considered. In this work, simulation is applied in two contexts: (1) to simulate the microscale pressure field based on experimentally-observed fluid configurations; and (2) to simulate two-fluid equilibrium configurations based on random initial conditions. Success with the first set of simulations in matching the experiments provides confidence that the results of the second set of computations represent physically reasonable configurations. Here we summarize each of the approaches.

10 Simulations are performed using a “color” lattice Boltzmann method (LBM). Our implementation has been described in detail in the literature (see McClure et al., 2014a, b). The approach relies on a multi-relaxation time (MRT) scheme to model the momentum transport. In the limit of low Mach number, the implementation recovers the Navier-Stokes equations with additional contributions to the stress tensor in the vicinity of the interfaces. The interfacial stresses between fluids result from capillary forces, which play a dominant role in many two-fluid porous medium systems. The formulation relies on separate
15 lattice Boltzmann equations (LBEs) to recover the mass transport for each fluid. This decouples the density from the pressure to allow for the simulation of incompressible fluids. Our implementation has been applied to simulate two-fluid-phase flows in a variety of porous medium geometries, recovering the correct scaling for common curve dynamics (McClure et al., 2016a), and it has also been used to closely predict experimental fluid configurations (Dye et al., 2015; Gray et al., 2015).

The implementation allows us to initialize fluid configurations directly from experimental images. Segmented images are generated from gray-scale camera data. These images were used to specify the initial position of the phases in the simulations with high resolution. The micromodel cell was computationally resolved within a domain that is $20 \times 500 \times 500$. The lattice spacing for the simulation was $\delta x = 1 \mu\text{m}$. Note that additional resolution was used to resolve the depth of the micromodel cell.



The physical depth of the simulation cell ($20 \mu\text{m}$) was larger than the depth of the micromodel cell ($4.4 \mu\text{m}$). This was done so
5 that the curvature in the depth of the cell could be resolved accurately. Due to geometric constraints, the curvature associated
with the micromodel depth cannot vary. The curvature of the interface between the two fluids can be written as

$$J_w = - \left(\frac{1}{R_1} + \frac{1}{R_2} \right), \quad (20)$$

where R_1 is the radius of curvature in the horizontal plane and R_2 is associated with the micromodel depth. Only R_1 can
vary independently. In the simulation, the fixed value of R_2 was $10 \mu\text{m}$. In the experiment, the fixed value of R_2 was 2.2
10 μm . With R_2 known in both cases, the simulated curvatures were mapped to the experimental system. In the experimental
system, pressure transducers were used to measure the phase pressures in the boundary reservoirs. These measurements were
used to inform pressure boundary conditions within the simulation. Since boundary conditions were enforced explicitly within
the simulation, the boundary pressures match the experimentally measured values exactly. The fluid configuration can vary
independently based on these conditions. Simulations were performed until the interfacial curvature stabilized, since prior
15 work has demonstrated the important fact that the curvature equilibrates more slowly compared to other macroscale quantities,
such as fluid saturation Gray et al. (2015).

A set of simulations was also performed based on random initial conditions. The approach used to generate random fluid
configurations and associated equilibrium states is described in detail by McClure et al. (2016b). The solid configuration for the
flow cell was identical for both sets of simulations. Blocks of fluid were inserted into the system at random until a desired fluid
20 saturation was obtained. This allowed for the generation of fluid configurations at wetting phase saturations that were below
the experimentally-determined irreducible wetting-phase saturation. Periodic boundary conditions were then enforced, and
the simulation was performed to produce an equilibrium configuration as determined by the average curvature of the interface
between fluids. Based on the final fluid configurations, connectivity-based analysis was performed to infer macroscale capillary
pressure, saturation, and interfacial area for a dense set of equilibrium states.

25 4.4 Results and Discussion

Phase connectivity presents a critical challenge for the theory and simulation of two-fluid-phase flow. When all or part of
a phase forms a fully-connected pathway through a porous medium, flow can occur without the movement of interfaces.
However, the case where phase sub-regions are not connected is a source of history-dependent behavior in traditional models.
Traditional models predict the capillary pressure as a function of the fluid saturation only, $p^c(s^{\overline{w}})$. However, this relationship is
30 not unique. Furthermore, key features of the relationship are an artifact of the experimental design. For example, the irreducible
wetting phase saturation, $s_I^{\overline{w}}$, can play an important role.

To calculate p^w as it is defined from Eq. 5, the microscale pressure field must be known throughout the domain. Simulation
provides a means to study how the pressure varies within the system and to obtain averages within all phase sub-regions.
Based on Eq. 16, values of p^{w_i} , $J_w^{w_i n}$ and $\epsilon^{\overline{w_i}}$ can be determined for each connected region of the wetting phase Ω_{w_i} for
 $i \in \{1, 2, \dots, N_w\}$. Two sets of simulations were performed, including (1) a set of 24 configurations initialized directly from
experimentally-observed configurations along primary drainage; and (2) a set of 48 configurations with random initial condi-

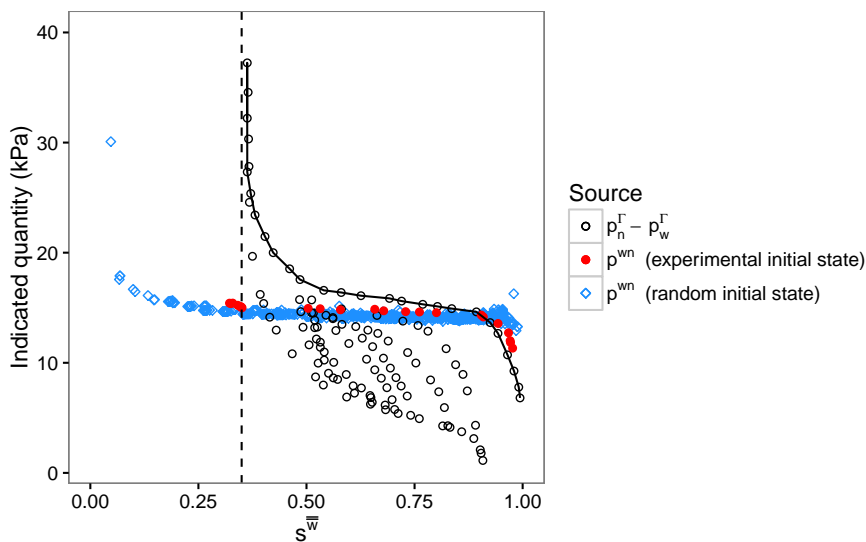


Figure 2. Comparison between the experimentally measured boundary pressure difference $p_n^\Gamma - p_w^\Gamma$ and the capillary pressure p^{wn} for the micromodel geometry. The solid line represents the boundary pressure along primary drainage.

tions as discussed in Section 4.3. The final fluid arrangements were analyzed to determine the true capillary pressure, p^{wn} , fluid saturation, \bar{s}_w , and specific interfacial area, \bar{c}^{wn} . The data was aggregated to produce a dense set of equilibrium configurations.

Pressure transducers located in each of the two fluid reservoirs were used to measure experimental boundary pressures for each fluid. The resulting values of $p_n^\Gamma - p_w^\Gamma$ are plotted in Fig. 2. Average capillary pressure values calculated from the simulations are presented along with this experimental data. The solid line represents the boundary pressure difference during primary drainage. The boundary pressures for simulations initialized from experimental data matched the experimentally measured values of $p_n^\Gamma - p_w^\Gamma$ exactly. Boundary measurements taken during simulation are also presented for imbibition and scanning curve sequences. The values of $p_n^\Gamma - p_w^\Gamma$ plotted in Fig. 2 represent a comprehensive set of experimental measurements that would typically be identified as capillary pressure values. This provides a basis for comparison with measurements of the true capillary pressure based on the configuration of the interfaces. In general, agreement between $p_n^\Gamma - p_w^\Gamma$ and p^{wn} should not be expected. Only when both the w and n fluids are fully connected and when the system is at equilibrium will the boundary pressure difference balance the internal average capillary pressure. The difference between the boundary measurement and the internal average capillary pressure is evident by comparing the experimental data from primary drainage and the simulation points initialized from the associated fluid configurations. Pressure boundary conditions for the simulations were set to match the measured values of p_n^Γ and p_w^Γ . As \bar{s}_w decreases, there is an increasing gap between $p_n^\Gamma - p_w^\Gamma$ and the average capillary pressure p^{wn} . This gap is attributed to the formation of disconnected wetting phase regions during drainage, an effect that is most significant as the irreducible wetting phase saturation is approached.



In the experimental system, the irreducible wetting phase saturation was clearly observed as $s_I^{\bar{w}} = 0.35$. This value is marked with a vertical dashed line in Fig. 2. The irreducible wetting phase saturation corresponds to the lowest experimentally accessible wetting phase saturation, since fluid configurations with $s^{\bar{w}} < s_I^{\bar{w}}$ cannot be obtained from the experimental setup. The underlying reason for this is related to the connectivity of the wetting phase. This can be understood from Fig. 3, which shows the phase configuration observed experimentally at the end of primary drainage. Within a connected region of wetting phase, the microscale pressure, p_w , will tend to be nearly constant. However, the wetting phase pressure can vary from one region to another. The connected components of the wetting phase are shown in Fig. 3 (b). At equilibrium, the measured difference in boundary pressures $p_n^\Gamma - p_w^\Gamma$ must balance with the capillary pressure of the interface sub-region between the two phase components. Note that the non-wetting phase is fully connected in Fig. 3 (a). The implication is that $p_n^\Gamma = p^n$ at equilibrium. However, p_w^Γ only reflects the pressure of the wetting phase reservoir. The sub-regions of the wetting phase that remain after primary drainage are plotted in color in Fig. 3 (b). The part of Ω_w that is connected to the wetting phase reservoir is shown in light green in Fig. 3 (b). When the irreducible wetting phase saturation is reached the portion of Ω_w that connects to the reservoir no longer fills any of the porespace within the micromodel. The irreducible wetting-phase saturation is associated with the trapped wetting phase regions only. Changing the pressure difference between the fluid reservoirs to increase $p_n^\Gamma - p_w^\Gamma$ does not change the capillary pressure in these regions. This leads to arbitrarily high measurements, claimed to be “capillary pressure” measurements, which are actually a difference in reservoir pressures rather than a measure of interface curvature. This also misconstrues the reduction in wetting phase saturation that occurs. The true average capillary pressure, as defined in Eq. 12, is much lower. Furthermore, the wetting-phase saturation can be further reduced as a consequence of other processes, such as evaporation. It is irreducible only within the context of the experimental design.

In light of this result, it is useful to consider alternative means to generate two-fluid configurations in porous media. For example, suppose a fluid configuration was encountered with $s^{\bar{w}} = 0.2$; how can we determine the macroscale capillary pressure? From a traditional macroscale parameterization approach, the experimentally proposed relation $p^{wn}(s^{\bar{w}})$ is of absolutely no use, since capillary pressure is undefined for $s^{\bar{w}} < s_I^{\bar{w}}$. From the microscale perspective, it is clearly possible to produce fluid configurations for which $s^{\bar{w}} < s_I^{\bar{w}}$ (for any system), and to measure the associated capillary pressure based on Eq. 12. For randomly initialized phase configurations, many such systems are produced. Simulations performed based on these initial geometries lead to equilibrium capillary pressure measurements shown in Fig. 2. While the classic “J curve” shape is still present, the experimentally-determined value $s_I^{\bar{w}}$ offers no guidance regarding this form.

Comparing capillary pressures measured from random initial conditions with those measured from experimental initial conditions provides additional insight. First, the true capillary pressure measurements based on Eq. 8 are remarkably consistent, particularly when considering the values of p^{wn} obtained as $s^{\bar{w}} \rightarrow s_I^{\bar{w}}$. Compared to randomly initialized data, configurations from primary drainage have a higher average capillary pressure. This is expected, since along primary drainage p^{wn} is determined by the pore-throat sizes. These represent the highest capillary pressures that are typically observed. We note that primary drainage does not specify the maximum possible capillary pressure, since bubbles of non-wetting phase may form that have a smaller radius of curvature than the minimum throat width.

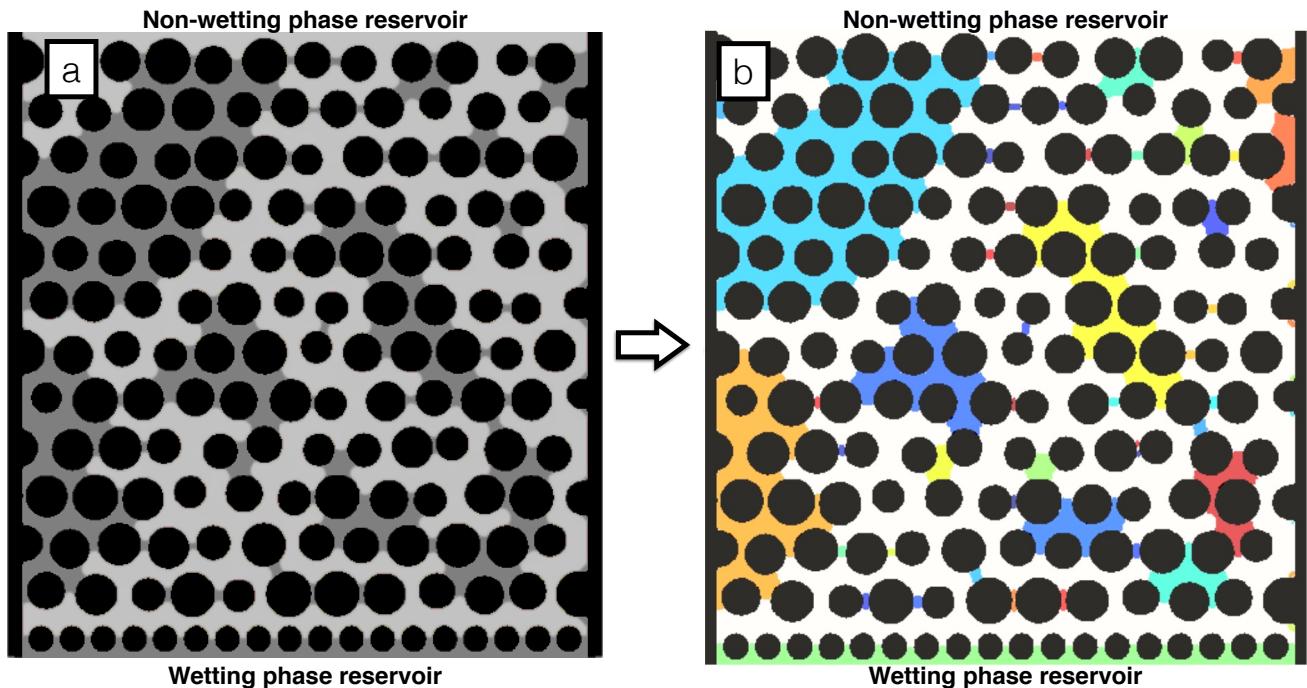


Figure 3. Phase connectivity has a direct impact on the meaning of the macroscale experimental measurements: (a) experimentally observed phase configuration corresponding to irreducible wetting phase saturation; and (b) connected components analysis shows all wetting phase that remains in the system is disconnected from the wetting phase reservoir. The black denotes the solid phase, the gray and various colors denote the wetting phase, and the white denotes the non-wetting phase.

Since the boundary pressure difference $p_n^\Gamma - p_w^\Gamma$ cannot be substituted for the capillary pressure, a key question is how this impacts capillary pressure hysteresis. When $p_n^\Gamma - p_w^\Gamma$ is used to erroneously infer the capillary pressure, the relationship between capillary pressure and saturation appears as the black circles in Fig. 2. When the true capillary pressure is used to plot the same data the shape of the relationship between capillary pressure and saturation is distinctly different. Capillary pressures are obtained at all fluid saturations, and no irreducible wetting-phase saturation is observed. Due to the fact that the true capillary pressure includes the effects of disconnected phase regions, moderate capillary pressures are observed. This is because the extrema for the boundary pressure measurements are not constrained by the internal geometry. We note that the relationship $p^{wn}(s^{\bar{w}})$ remains non-unique. The higher-dimensional form $p^{wn}(s^{\bar{w}}, \epsilon^{\bar{wn}})$ is therefore considered in Fig. 4.

Using a generalized additive model (GAM), a best-fit surface was generated to approximate the simulated data, incorporating data points derived from both random and experimentally-observed initial conditions. The black lines in Fig. 4 show the iso-contours of the capillary pressure surface (p^{wn} is constant along each contour). It is clear that primary drainage leads to states with lower interfacial area as compared to randomly initialized configurations. Both sets of points lie along a consistent

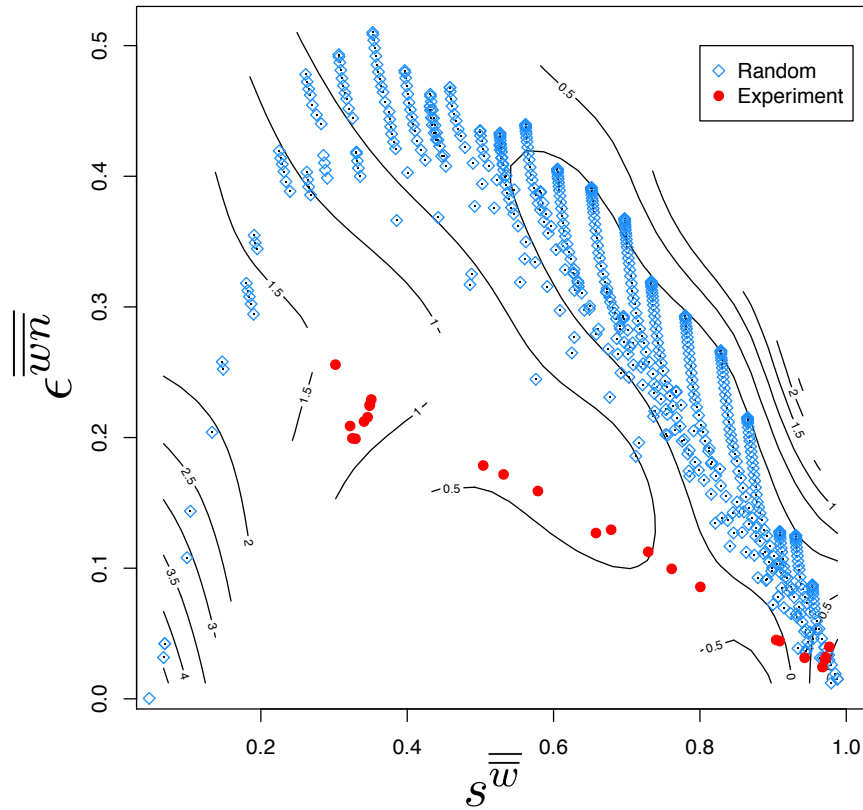


Figure 4. Contour plot showing the relationship $p^{wn}(\overline{s^w}, \overline{\epsilon^{wn}})$, with the black curves representing constant value of p^{wn} . Data points used to construct the surface are also shown, including randomly initialized fluid configurations (blue) and experimentally initialized configurations from primary drainage (red).

surface. The extent to which the relationships $p^{wn}(\overline{s^w})$ and $p^{wn}(\overline{s^w}, \overline{\epsilon^{wn}})$ describe the data points measured from microscale configurations are quantitatively assessed by evaluating the residuals for the GAM approximation. The residuals are shown in Fig. 5. The traditionally used relationship $p^{wn}(\overline{s^w})$ is able to explain only 60.6% of the variance in the data. When the effect of interfacial area is included, $p^{wn}(\overline{s^w}, \overline{\epsilon^{wn}})$, 77.1% of the variance is explained. Based on previous work for three-dimensional porous media, it is anticipated that higher fidelity approximations can be produced by including the effects of other topological invariants, such as the average Gaussian curvature or Euler characteristic (McClure et al., 2016b).

5 Conclusions

In this work, we show that the ability to quantitatively analyze the internal structure of two-fluid porous medium systems has a profound impact on macroscale understanding. We considered the behavior of the capillary pressure based on traditional

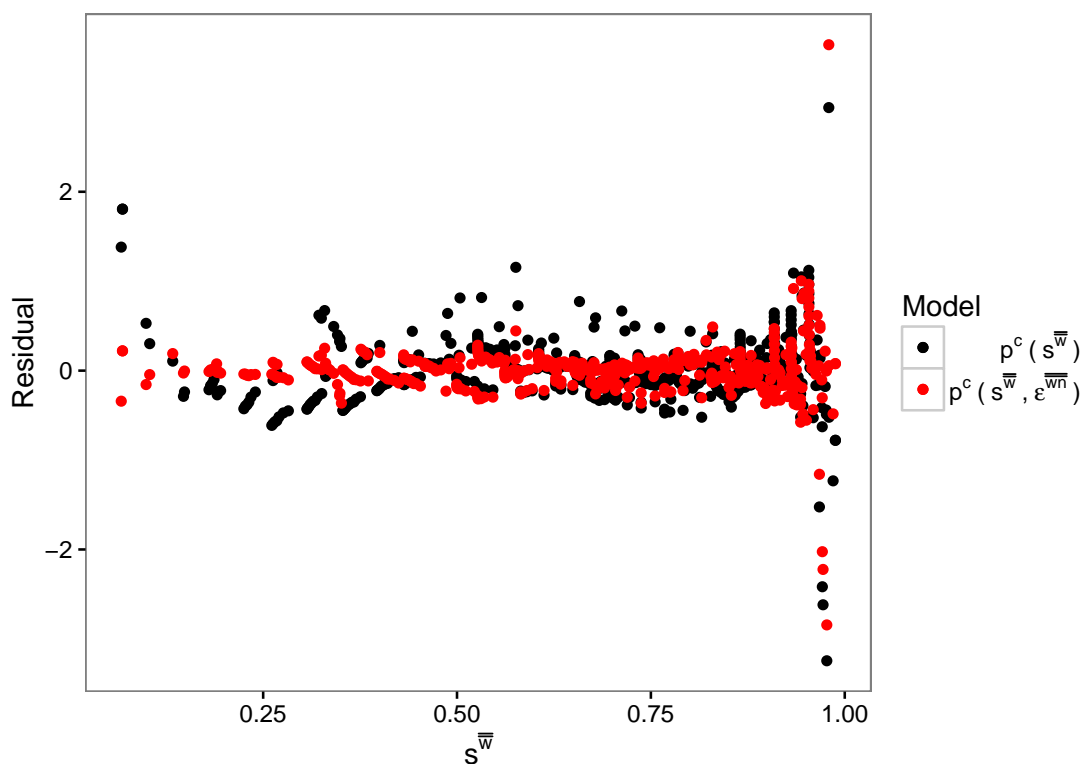


Figure 5. Comparison of the residual errors for the GAM fits that approximate $p^{wn}(s_w)$ and $p^{wn}(s_w, \epsilon_w)$.

laboratory boundary measurements and compare to the true average capillary pressure, a state function, determined by directly averaging the curvature of the interface between fluids. We demonstrate that the difference between the phase pressures as measured from the boundary cannot be used to deduce the capillary pressure of the system. In particular, the high capillary pressure measured for irreducible wetting phase saturation is an artifact of the experimental design. Four important conclusions result.

First, the true capillary pressure measured at irreducible wetting-phase saturation is significantly lower than predicted from boundary pressure measurements. This can be understood based on the underlying phase connectivity. At irreducible wetting-phase saturation the wetting-phase reservoir pressure no longer reflects the internal pressure of the system, since the reservoir does not connect to the remaining wetting phase inside the system.

Second, randomly generated fluid configurations provide a way to access states where the wetting-phase saturation is below the irreducible wetting phase saturation. By carrying out direct averaging based on these states, the capillary pressure state function can be studied over the full range of possible saturation values, including configurations that are inaccessible from traditional experiments. We note that modified experimental designs could be used to accomplish the same objective.



5 Third, we show that the equilibrium relationship between capillary pressure, fluid saturation and interfacial area is consistent between randomly and experimentally initialized configurations. Combining the two data sets, generalized additive models were used to approximate the surface relating the three quantities. At fixed saturation, states from primary drainage have higher capillary pressure and lower interfacial area compared to randomly generated states. Our results are particularly significant for systems where low wetting-phase configurations are important, such as evaporation in the vadose zone.

10 Fourth, this analysis demonstrates the importance of understanding the essence of capillary pressure. The term “dynamic capillary pressure” has unfortunately made its way into the literature where this quantity is the evolving value of a pressure difference between phases or of the difference between boundary pressures. In fact, capillary pressure is a state function, as are the pressures of each phase, that is defined without reference to or knowledge of the fluid pressures in the phases. System dynamics cause a relation among pressures to relax toward satisfaction of Laplace’s law at equilibrium, but none of the pressures in this relation rely on this balance for their definition.

15 *Author contributions.* All authors participated in the writing of this manuscript. WGG and CTM contributed to the introduction, background, and theory, ALD contributed to the microfluidics, and JEM contributed to lattice Boltzmann modeling. All authors contributed to the discussion and conclusions from this work.

Acknowledgements. This work was supported by Army Research Office grant W911NF-14-1-02877, Department of Energy grant DE-SC0002163, and National Science Foundation grant 1619767. An award of computer time was provided by the Department of Energy INCITE program. This research also used resources of the Oak Ridge Leadership Computing Facility, which is a DOE Office of Science User Facility supported under Contract DE-AC05-00OR22725.



References

- Albers, B.: Modeling the hysteretic behavior of the capillary pressure in partially saturated porous media: a review, *Acta Mechanica*, 225, 2163–2189, 2014.
- Alizadeh, A. H. and Piri, M.: The effect of saturation history on three-phase relative permeability: An experimental study, *Water Resources Research*, 50, 1636–1664, 2014.
- Anderson, T. B. and Jackson, R.: A fluid mechanical description of fluidized beds, *Industrial and Engineering Chemistry Fundamentals*, 6, 527–539, 1967.
- Bachmat, Y. and Bear, J.: The General Equations of Hydrodynamic Dispersion in Homogeneous, Isotropic, Porous Mediums, *Journal of Geophysical Research*, 69, 2561–2567, 1964.
- 15 Bauer, P., Thorpe, A., and Brunet, G.: The quiet revolution of numerical weather prediction, *Nature*, 525, 47–55, 2015.
- Bear, J.: *Dynamics of Fluids in Porous Media*, Elsevier, New York, 1972.
- Bernard, P. S. and Wallace, J. M.: *Turbulent Flow*, John Wiley & Sons, 2002.
- Blöschl, G.: Scaling in Hydrology, *Hydrological Processes*, 15, 709–711, 2001.
- Blöschl, G., Grayson, R. B., and Sivapalan, M.: On the representative elementary area (rea) concept and its utility for distributed rainfall-runoff modelling, *Hydrological Processes*, 9, 313–330, 1995.
- 20 Bradshaw, P.: *An Introduction to Turbulence and its Measurement*, Pergamon Press, 1971.
- Chanson, H.: Current knowledge in hydraulic jumps and related phenomena. A survey of experimental results, *European Journal of Mechanics B Fluids*, 28, 191–210, 2009.
- Collins, R., Triplett, C., Barjatya, A., Lehmacher, G., and Fritts, D.: Using lidar and rockets to explore turbulence in the atmosphere, *SPIE Newsroom*, doi:10.1117/2.1201505.005922, 2015.
- 25 Cushman, J. H.: *The Physics of Fluids in Hierarchical Porous Media: Angstroms to Miles*, Kluwer Academic Publishers, Dordrecht, The Netherlands, 1997.
- D’Asaro, E. A.: Turbulence in the Upper-Ocean Mixed Layer, *Annual Review of Marine Science*, 6, 101–115, 2014.
- Deems, J. S., Painter, T. H., and Finnegan, D. C.: Lidar measurement of snow depth: a review, *Journal of Glaciology*, 59, 467–479, 2013.
- 30 Dietrich, J. C., Dawson, C. N., Proft, J. M., Howard, M. T., Wells, G., Fleming, J. G., Luettich Jr., R. A., Westerink, J. J., Cobell, Z., Vitse, M., Lander, H., Blanton, B. O., Szpilka, C. M., and Atkinson, J. H.: Real-time forecasting and visualization of hurricane waves and storm surges using SWAN+ADCIRC and FigureGen, in: *Computational Challenges in the Geosciences*, edited by Dawson, C. and Gerritsen, M., vol. 156 of *The IMA Volumes in Mathematics and Its Applications*, Springer Science & Business Media, New York, 2013.
- Dudhia, J.: A history of mesoscale model development, *Asia-Pacific Journal of Atmospheric Science*, 50, 121–131, 2014.
- 35 Dye, A. L., McClure, J. E., Gray, W. G., and Miller, C. T.: Multiscale modeling of porous medium systems, in: *Handbook of Porous Media*, edited by Vafai, K., chap. 1, pp. 3–45, CRC Press, third edn., 2015.
- Essex, C., McKittrick, R., and Andresen, B.: Does a Global Temperature Exist?, *Journal of Non-Equilibrium Thermodynamics*, 32, 1–27, 2007.
- Flint, L. E., Flint, A. L., Thorne, J. H., and Boynton, R.: Fine-scale hydrologic modeling for regional landscape application: the California Basin characterization model development and performance, *Ecological Processes*, 2, <http://www.ecologicalprocesses.com/content/2/1/25>, 2013.
- 5



- Fuentes, F. C., Iungo, G. V., and Porté-Agel, F.: 3D turbulence measurements using three synchronous wind lidars: Validation against sonic anemometry, *Journal of Atmospheric and Oceanic Technology*, 31, 1549–1556, 2014.
- Gentine, P., Troy, T. J., Lintner, B. R., and Findell, K. L.: Scaling in Surface Hydrology: Progress and Challenges, *Journal of Contemporary Water Research & Education*, 147, 28–40, 2012.
- 10 Gleeson, T. and Paszkowski, D.: Perceptions of scale in hydrology: What do you mean by regional scale?, *Hydrological Sciences Journal*, doi:10.1080/02626667.2013.797581, 2014.
- Gray, W. G. and Miller, C. T.: A generalization of averaging theorems for porous medium analysis, *Advances in Water Resources*, 62, 227–237, doi:10.1016/j.advwatres.2013.06.006, 2013.
- Gray, W. G. and Miller, C. T.: *Introduction to the Thermodynamically Constrained Averaging Theory for Porous Media Systems*, Springer-
15 Verlag, 2014.
- Gray, W. G. and O'Neill, K.: On the development of Darcy's law for the general equations for flow in porous media, *Water Resources Research*, 12, 148–154, 1976.
- Gray, W. G., Dye, A. L., McClure, J. E., Pyrak-Nolte, L. J., and Miller, C. T.: On the dynamics and kinematics of two-fluid-phase flow in porous media, *Water Resources Research*, 51, 5365–5381, 2015.
- 20 Hermann, S. M. and Sop, T. K.: The map is not the territory: How satellite remote sensing and ground evidence have re-shaped the image of Sahelian desertification, in: *The End of Desertification? Disputing Environmental Change in the Drylands*, edited by Behnke, R. and Mortimore, M., Springer Earth System Sciences, pp. 117–145, Springer, 2016.
- Hornung, U.: *Homogenization and Porous Media*, no. 6 in *Interdisciplinary Applied Mathematics*, Springer, 1997.
- Ishii, M., Kim, S., and Kelly, J.: Development of Interfacial Area Transport Equation, *Nuclear Engineering and Technology*, 37, 525–536,
25 2005.
- Kauffeldt, A., Halldin, S., Rodhe, A., Xu, C.-Y., and Westerberg, I. K.: Disinformative data in large-scale hydrological modelling, *Hydrology and Earth System Sciences*, 17, 2845–2857, 2013.
- Kauffeldt, A., Wetterhall, F., Pappenberger, F., Salamon, P., and Thielen, J.: Technical review of large-scale hydrological models for implementation in operational flood forecasting schemes on continental level, *Environmental Modelling and Software*, 75, 68–76, 2016.
- 30 Knödel, K., Lange, G., and Voigt, H.-J.: *Environmental Geology: Handbook of Field Methods and Case Studies*, Springer Berlin Heidelberg New York, 2007.
- Kocamustafaogullari, G. and Ishii, M.: Foundation of the interfacial area transport equation and its closure relations, *International Journal of Heat and Mass Transfer*, 38, 481–493, 1995.
- Lillesand, T. M., Kiefer, R. W., and Chipman, J. W.: *Remote Sensing and Image Interpretation*, Wiley, seventh edn., 2015.
- 35 Ly, S., Charles, C., and Degré, A.: Different methods for spatial interpolation of rainfall data for operational hydrology and hydrological modeling at watershed scale. A review, *Biotechnology, Agronomy, Society and Environment*, 17, 392–406, 2013.
- Marle, C.: Écoulements monophasiques en milieu poreux, *Revue de L'Institut Français du Pétrole*, 22, 1471–1509, 1967.
- Maugin, G. A.: *The Thermomechanics of Nonlinear Irreversible Behaviors: An Introduction*, World Scientific Press, Singapore, 1999.
- McClure, J. E., Berrill, M. A., Gray, W. G. and Miller, C. T.: Tracking Interface and Common Curve Dynamics for Two-Fluid Flow in Porous Media, *Journal of Fluid Mechanics*, 796, 211–232, 2016a.
- McClure, J. E., Berrill, M. A., Gray, W. G. and Miller, C. T.: Influence of phase connectivity on the relationship among capillary pressure,
5 fluid saturation, and interfacial area in two-fluid-phase porous medium systems, *Physical Review E*, (Accepted), 2016b.



- McClure, J. E., Prins, J. F., and Miller, C. T.: A Novel Heterogeneous Algorithm to Simulate Multiphase Flow in Porous Media on Multicore CPU-GPU Systems, *Computer Physics Communications*, 185, 1865–1874, doi:<http://dx.doi.org/10.1016/j.cpc.2014.03.012>, 2014a.
- McClure, J. E., Wang, H., Prins, J. F., Miller, C. T., and Feng, W.: Petascale Application of a Coupled CPU-GPU Algorithm for Simulation and Analysis of Multiphase Flow Solutions in Porous Medium Systems, in: 28th IEEE International Parallel & Distributed Processing Symposium, Phoenix, Arizona, 2014b.
- 10 Miller, C. T., Christakos, G., Imhoff, P. T., McBride, J. F., Pedit, J. A., and Trangenstein, J. A.: Multiphase flow and transport modeling in heterogeneous porous media: Challenges and approaches, *Advances in Water Resources*, 21, 77–120, 1998.
- Miller, C. T., Dawson, C. N., Farthing, M. W., Hou, T. Y., Huang, J. F., Kees, C. E., Kelley, C. T., and Langtangen, H. P.: Numerical simulation of water resources problems: Models, methods, and trends, *Advances in Water Resources*, 51, 405–437, doi:10.1016/j.advwatres.2012.05.008, 2013.
- 15 Miller, C. T., Christakos, G., Imhoff, P. T., McBride, J. F., Pedit, J. A., and Trangenstein, J. A.: Multiphase flow and transport modeling in heterogeneous porous media: Challenges and approaches, *Advances in Water Resources*, 21, 77–120, 1998.
- Nickerson, C., Harper, M., Henrie, C. J., Mayberry, R., Shimmin, S., Smith, B., and Smith, J. H.: Sources of Data Providing Land Use and Land Cover Estimates for the U. S., Tech. rep., Interagency Council on Agricultural and Rural Statistics, subcommittee of the Interagency Council on Statistical Policy, <https://www.data.gov/media/2013/10/attachments/ICARS%20Land%20Use%20and%20Cover%20data.pdf>, 2013.
- 20 Niessner, J., Berg, S., and Hassanizadeh, S. M.: Comparison of Two-Phase Darcy's Law with a Thermodynamically Consistent Approach, *Transport in Porous Media*, 88, 133–148, doi:10.1007/s11242-011-9730-0, 2011.
- Paiva, R. C. D., Collischonn, W., and Tucci, C. E. M.: Large scale hydrologic and hydrodynamic modeling using limited data and a GIS based approach, *Journal of Hydrology*, 406, 170–181, 2011.
- 25 Panfilov, M.: *Macroscale Models of Flow Through Highly Heterogeneous Porous Media*, Springer, 2000.
- Pechlivanidis, I. G., Jackson, B. M., McIntyre, N. R., and Wheeler, H. S.: Catchment scale hydrological modelling: A review of model types, calibration approaches and uncertainty analysis methods in the context of recent developments in technology and applications, *Global NEST Journal*, 13, 193–214, 2011.
- 30 Reggiani, P., Sivapalan, M., and Hassanizadeh, S. M.: A Unifying Framework for Watershed Thermodynamics: Balance Equations for Mass, Momentum, Energy and Entropy, and the Second Law of Thermodynamics, *Advances in Water Resources*, 22, 367–398, 1998.
- Reggiani, P., Hassanizadeh, S. M., Sivapalan, M., and Gray, W. G.: A Unifying Framework for Watershed Thermodynamics: Constitutive Relationships, *Advances in Water Resources*, 23, 15–39, 1999.
- Sathe, A. and Mann, J.: A review of turbulence measurements using ground-based wind lidars, *Atmospheric Measurement Techniques*, 6, 3147–3167, 2013.
- 35 Skøien, J. O., Blöschl, G., and Western, A. W.: Characteristic space scales and timescales in hydrology, *Water Resources Research*, 39, 11–11–19, 2003.
- Vreugdenhil, C. B.: *Numerical Methods for Shallow-Water Flow*, no. 13 in *Water Science and Technology Library*, Springer, 1995.
- Wang, A., Zeng, X., Shen, S. S. P., Zeng, Q.-C., and Dickinson, R. E.: Time Scales of Land Surface Hydrology, *Journal of Hydrometeorology*, 7, 868–879, 2006.
- Whitaker, S.: *Diffusion and Dispersion in Porous Media*, *American Institute of Chemical Engineers Journal*, 13, 420–427, 1967.
- Whitaker, S.: *Flow in Porous Media I: A Theoretical Derivation of Darcy's Law*, *Transport in Porous Media*, 1, 3–25, 1986.
- 5 Whitaker, S.: *The Method of Volume Averaging*, Kluwer Academic Publishers, Dordrecht, 1999.



- Wildenschild, D. and Sheppard, A. P.: X-ray imaging and analysis techniques for quantifying pore-scale structure and processes in subsurface porous medium systems, *Advances in Water Resources*, 51, 217–246, 2013.
- 545 Wood, E. F.: Scaling behaviour of hydrological fluxes and variables: Empirical studies using a hydrological model and remote sensing data, *Hydrological Processes*, 9, 331–346, 1995.
- Wood, E. F., Sivapalan, M., Beven, K., and Band, L.: Effects of spatial variability and scale with implications to hydrologic modeling, *Journal of Hydrology*, 102, 29–47, 1988.
- Zhou, Y. and Li, W.: A review of regional groundwater flow modeling, *Geoscience Frontiers*, 2, 205–214, 2011.